


DOI 10.24425/ae.2023.146048

# Train based on virtual synchronous generator technology uninterrupted phase-separation passing study

YING WANG, HUAN YANG , XIAOQIANG CHEN, YA GUO

*School of Automation and Electrical Engineering, Lanzhou Jiaotong University  
Lanzhou, 730070, China*

*e-mail: wangying01@lztu.edu.cn, mr.braveyang@foxmail.com*

(Received: 12.03.2023, revised: 30.05.2023)

**Abstract:** The problem of large speed loss exists in the traditional passing through the electric phase-separation method of trains, which is more prominent when trains pass through an electric phase-separation zone in the uphill section of long ramps and may lead to the trains not passing through the phase-separation zone safely. In order to solve this problem, based on the energy storage type railroad power conditioner, a train uninterrupted phase-separation passing system based on the energy storage type railroad power conditioner is proposed. The energy storage railroad power conditioner can realize the recovery and utilization of regenerative braking energy of the electrified railroad. In the structure of the energy storage railroad power conditioner, the single-phase inverter is led from the middle DC side of the energy storage railroad power conditioner and connected to the neutral line through the LCL filter and the step-up transformer, which constitutes an uninterrupted phase-separation passing system. The single-phase inverter is controlled using virtual synchronous generator technology, which allows the single-phase inverter to have external characteristics similar to those of a synchronous generator, providing support for the voltage and frequency in the neutral zone. The power required by the train to pass the electric phase-separation is provided by the power supply arm or the energy storage system, which not only improves the utilization rate of regenerative braking energy but also realizes the uninterrupted phase-separation passing of the train through the control of the voltage in the neutral region.

**Key words:** energy storage railway power conditioner, single-phase inverter, uninterrupted phase-separation passing, virtual synchronous generator



© 2023. The Author(s). This is an open-access article distributed under the terms of the Creative Commons Attribution-NonCommercial-NoDerivatives License (CC BY-NC-ND 4.0, <https://creativecommons.org/licenses/by-nc-nd/4.0/>), which permits use, distribution, and reproduction in any medium, provided that the Article is properly cited, the use is non-commercial, and no modifications or adaptations are made.

## 1. Introduction

The terrain in the western region of China is complex, mostly plateaus, mountains, and basins, and the terrain is undulating, making railroad construction very difficult. In order to avoid bad geology, overcome plateau obstacles, reduce construction difficulties, and save project investment, the railroad construction process needs to use larger slopes and longer slope sections, abbreviated as long ramps. Due to the long ramp section, more inevitably will be set in the long slope section electric phase. At present, China's high-speed railroads are generally set up every twenty to thirty kilometers at an electric phase-separation, and the trains need to rely on inertia to pass through the "electric phase-separation" [1]. When there is an electric phase-separation in the uphill section of the long gradient, when the moving train idles through the electric phase-separation, due to the large gradient slope resistance, it may cause the train to slow down too much, and may even cause the entrance speed is too low to idle through the powerless area, resulting in a slope stop accident, affecting the safe and reliable operation of the train [2]. To solve this problem, it can be considered that the train is uninterrupted phase-separation passing (UPSP) in the long ramp section.

Regarding the problem of uninterrupted phase-separation passing of trains, scholars at home and abroad have proposed a variety of solutions for uninterrupted phase-separation passing. The existing solutions mainly include the UPSP technology [3], the same phase power supply technology [4], and the medium voltage DC traction power supply technology [5]. Among them, both the same-phase power supply technology and the medium voltage DC traction power supply technology require the large-scale transformation of the existing traction power supply system, which is not conducive to the popularization and application of the existing lines. Therefore, it is of great practical significance to study the train's non-stop power splitting technology without changing the structure of the existing traction power supply system to achieve high-speed, heavy-duty operation of trains and give full play to the capacity of existing lines.

References [6, 7] proposed setting up a converter in the electric phase separation area so that the neutral section voltage can be flexibly transitioned between the two supply arms to realize the train's uninterrupted phase-separation passing. Reference [8] changed the neutral line voltage phase by means of a railway power regulator (RPC) and a phase-shifting transformer in series so that the train can have uninterrupted phase-separation passing. In Reference [9], a single-phase inverter is connected in series with a phase-shifting transformer through the middle DC side of the railway power regulator to eliminate the dead zone of the power supply in the electrical phase-separation link. In References [10–12], with the continuous maturity of railroad power conditioners, some scholars proposed the energy storage railroad power conditioner, which can recover and utilize the braking energy generated during the braking process of the train. On this basis, this paper proposes a single-phase inverter leading from the middle DC side of the energy-storage railway power conditioner, which is connected to the neutral zone via an LCL filter and step-up transformer for a constant power splitting system. The energy storage medium is a supercapacitor, and the DC/DC converter forms a supercapacitor energy storage system (SCESS). The railroad power regulator and the supercapacitor energy storage system constitute the RPC–SCESS. In References [13–15], by using the virtual synchronous generator (VSG) control technology to make the single-phase inverter with synchronous generator-like characteristics, the power required by the train to over-phase can be provided by the energy

storage system, and by controlling the phase of the single-phase VSG output voltage, the train can be flexibly and uninterrupted phase-separation passing in the neutral zone. It also improves the regenerative braking energy utilization.

## 2. Analysis of RPC–SCESS-based UPSP system

### 2.1. Topology of RPC–SCESS-based UPSP system

Based on the RPC–SCESS uninterrupted phase-separation passing system as shown in Fig. 1, The UPSP system consists of a single-phase inverter, LCL filter, and step-up transformer.  $I_a$ ,  $I_b$ , and  $I_c$ , respectively, represent the three-phase current on the primary side of the V/v traction transformer.  $I_\alpha$  and  $I_\beta$  are the load current of the two supply arms.  $L_s$  is the filter inductance.  $U_{dc}$  is the intermediate DC side voltage of the RPC–SCESS.  $C_d$  is composed of  $C_1$  and  $C_2$  in series.

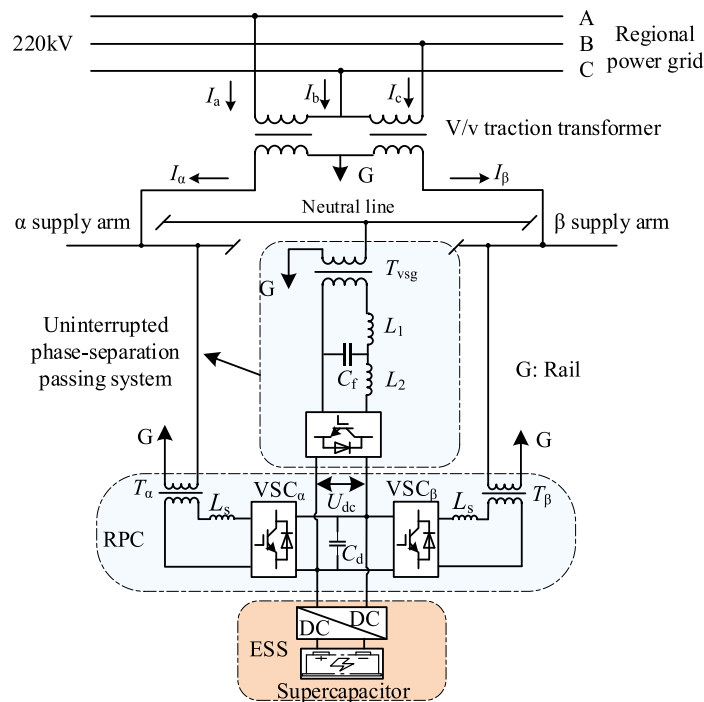


Fig. 1. Schematic diagram of UPSP system based on RPC–SCESS

### 2.2. Power flow analysis

In order to prevent the energy storage system from overcharging and over-discharging, the state of charge (SOC) interval of the energy storage system is set to 0.1–0.95. When the train is over electric phase-separation, it can be divided into two working conditions, the first working condition is that the state of charge of the energy storage system is not in the working interval,

and the second working condition is that the state of charge of the energy storage system is in the working interval. The power flow analysis when continuously passing through the electric phase-separation is shown in Fig. 2.

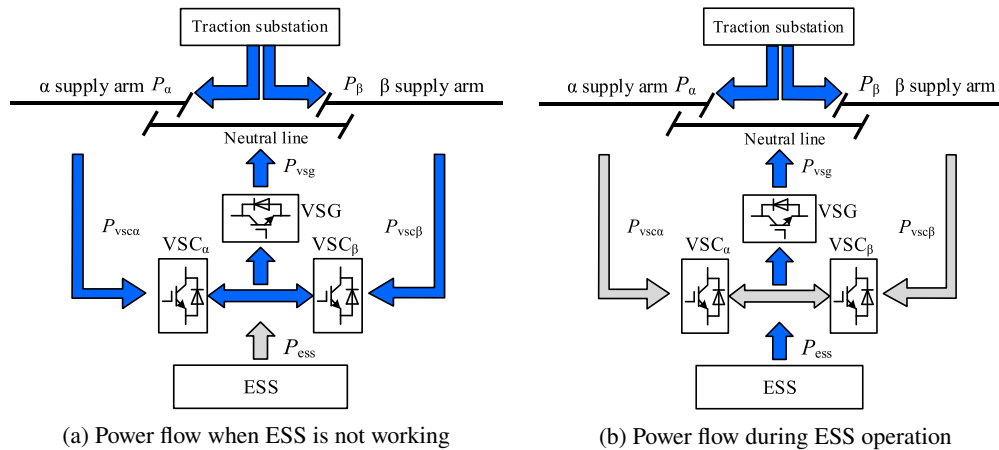


Fig. 2. Analysis of train uninterrupted phase-separation passing power flow

The first working condition of the train past the electric phase-separation power flow is shown in Fig. 2(a), when the charge state of the energy storage system is not in the working interval, the energy storage system does not work, and the power required by the train over-phase is provided by the two power supply arms at this time. The single-phase inverter output power is the sum of the left and right converter transmission power of the railroad power conditioner.

$$P_{vsg} = P_{vsg\alpha} + P_{vsg\beta}, \quad P_{vsg\alpha} = P_{vsg\beta}. \quad (1)$$

The second working condition of the train passing the electric phase-separation power flow is shown in Fig. 2(b), where the power required by the train over-phase is provided by the supercapacitor energy storage system. At this time, the single-phase inverter output power is equal to the energy storage system output power, as shown in the following simple form:

$$P_{vsg} = P_{ess}. \quad (2)$$

### 3. UPSP control strategy based on RPC–SCCESS

#### 3.1. RPC–SCCESS control strategy

The effective value of fundamental compensation current provided by the RPC–SCCESS to  $\alpha$  and  $\beta$  power supply arms can be expressed as:

$$\begin{cases} I_{\alpha c} = \sqrt{\left[-0.5(I_{L\alpha p} - I_{L\beta p}) + 0.5(I_{st\alpha} + I_{st\beta})\right]^2 + \left[-I_{L\alpha q} - \frac{\sqrt{3}}{3}(I_{L\alpha p} + I_{\alpha cp})\right]^2} \\ I_{\beta c} = \sqrt{\left[0.5(I_{L\alpha p} - I_{L\beta p}) + 0.5(I_{st\alpha} + I_{st\beta})\right]^2 + \left[-I_{L\beta q} + \frac{\sqrt{3}}{3}(I_{L\beta p} + I_{\beta cp})\right]^2} \end{cases} \quad (3)$$

$I_{L\alpha p}$  and  $I_{L\beta p}$  are the active components of compensating preload current  $i_{L\alpha}$  and  $i_{L\beta}$ .  $I_{L\alpha q}$  and  $I_{L\beta q}$  are the reactive components of compensating preload current  $i_{L\alpha}$  and  $i_{L\beta}$ .  $I_{st\alpha}$  and  $I_{st\beta}$  are the active currents compensated by the SCESS on the two supply arms.  $I_{\alpha cp}$  and  $I_{\beta cp}$  are the active currents compensated by the RPC.

When there is a train passing the electric phase separation, the compensation current of the SCESS is shown in Eq. (4), and  $U_{sc}$  is the terminal voltage of the supercapacitor.

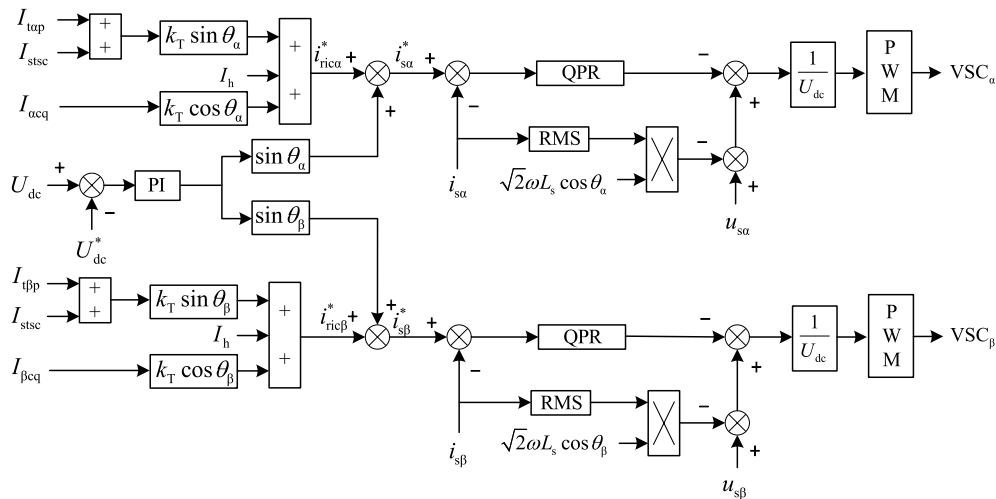
$$I_{stsc} = \frac{P_{vsg}}{U_{sc}} \quad (4)$$

Traction network low harmonics are mainly concentrated in 3, 5, 7, 9 times, higher harmonics are mainly concentrated in 43, 44, 47, 49, 51, and 53 times [16], ignore the other every harmonic and at this point, the traction network characteristic harmonic current as shown in following form:

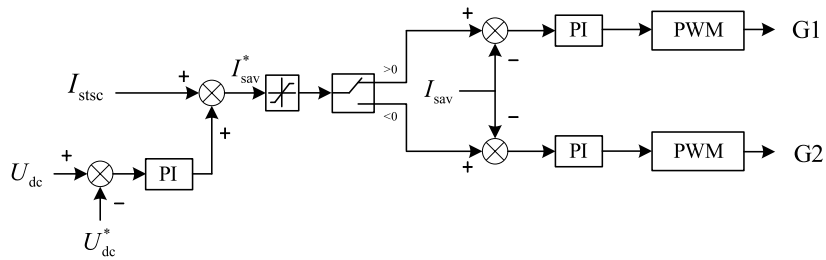
$$i_h = \sum_{h=3,\dots,9} \sqrt{2}I_h \sin(h\omega t + \varphi_h) + \sum_{h=43,\dots,53} \sqrt{2}I_h \sin(h\omega t + \varphi_h) \quad (5)$$

The control strategy of the RPC–SCESS is shown in Fig. 3,  $I_{\alpha cp}$  and  $I_{\beta cp}$  are the active currents transmitted by the RPC.  $I_{\alpha cq}$ ,  $I_{\beta cq}$  are the reactive currents compensated by the RPC.

In Fig. 3, the control strategy of the RPC–SCESS is divided into two parts: RPC control strategy and SCESS control strategy.  $I_{sav}$  is the actual current of the ESS.  $I_{s\alpha}$  and  $I_{s\beta}$  are the actual output current of the two converters.  $u_{s\alpha}$  and  $u_{s\beta}$  are the AC port voltages of the two converters.



(a) RPC control strategy



(b) SCESS control strategy

Fig. 3. RPC–SCESS control strategy

Quasi proportional resonant (QPR) controller is used for accurate current tracking [17]. The RPC–SCESS control strategy can realize the negative sequence compensation of the power supply arm, balance the active power, recover the braking energy of the power supply arm, and keep the intermediate DC side voltage stable.

### 3.2. UPSP control strategy

The UPSP control strategy based on a single-phase VSG requires the establishment of mathematical models to simulate the output characteristics of synchronous generators. In modeling VSGs, the second-order synchronous motor model considering rotor inertia and damping factors is widely used in various VSG schemes [18–21]. The second-order synchronous motor model is shown in the following equations:

$$J \frac{d\omega}{dt} = T_m - T_e - T_d = T_m - T_e - D_p(\omega - \omega_0), \quad (6)$$

$$\frac{d\theta}{dt} = \omega. \quad (7)$$

In Eqs. (6) and (7),  $J$  represents the moment of inertia.  $T_m$ ,  $T_e$ , and  $T_d$ , respectively, represent the mechanical torque, electromagnetic torque, and damping torque of the synchronous motor. Here,  $\omega$  represents the actual angular frequency,  $\omega_0$  represents the rated angular frequency,  $D_p$  represents the damping coefficient, and  $\theta$  represents the angular displacement of the motor rotor.

According to the second-order model of synchronous motors, it is necessary to establish the mathematical models of virtual  $T_m$ ,  $T_e$  and  $T_d$  to make a single-phase inverter have the external characteristics of a generator. The mathematical model of a single-phase VSG is:

$$T_m = \frac{P_{set}}{\omega_0}, \quad (8)$$

$$T_d = D_p(\omega - \omega_0), \quad (9)$$

$$T_e = M_f i_f i_{vsg} \sin \theta, \quad (10)$$

$$e = M_f i_f \omega \sin \theta, \quad (11)$$

$$P_{vsg} = \omega T_e = \omega M_f i_f i_{vsg} \sin \theta, \quad (12)$$

$$Q_{vsg} = -\omega M_f i_f i_{vsg} \cos \theta. \quad (13)$$

It can be seen from Eqs. (10), (12) and (13) that  $T_e$ ,  $P_{vsg}$ , and  $Q_{vsg}$  contain double-frequency components, so filtering should be added during modeling. The order of the filter has a greater impact on the system. The higher the order, the slower the dynamic response speed, which is not conducive to the fast-tracking of  $P_{vsg}$  and  $Q_{vsg}$ . The moving average filter (MAF) [22] is adopted to filter  $T_e$  and  $Q_{vsg}$  to improve the rapid response of the system. The specific control block diagram based on single-phase VSG continuous current transition is shown in Fig. 4.

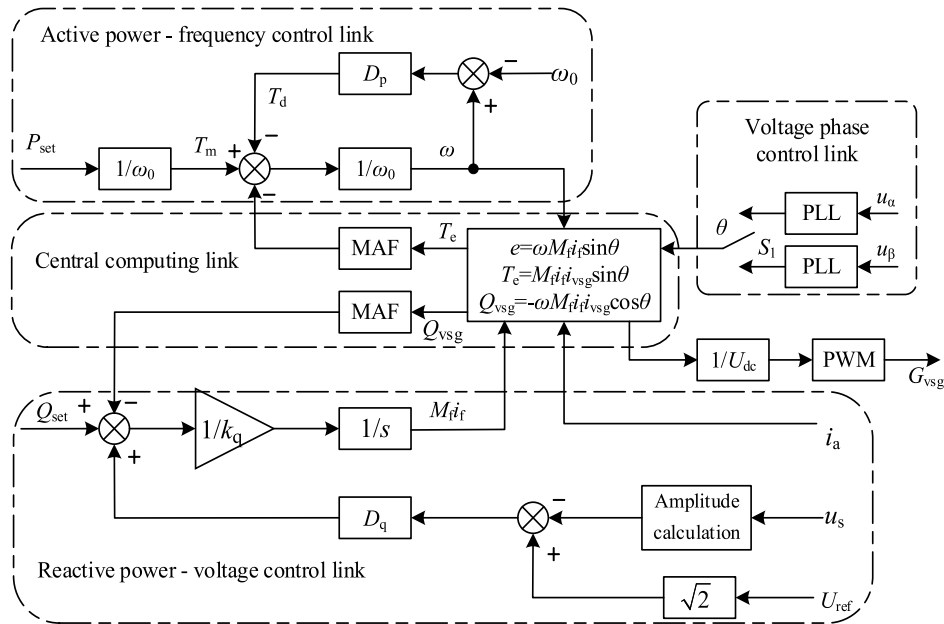


Fig. 4. Based on single phase VSG continuous current phase control block diagram

In Fig. 4, the UPSP control strategy based on a single-phase VSG is divided into four parts, which are the active power-frequency control link, central calculation link, reactive power-voltage control link, and voltage phase control link.  $P_{set}$  and  $Q_{set}$  are the target values of single-phase VSG power output. In this paper,  $P_{set}$  and  $Q_{set}$  are set to zero. The output power of a single-phase VSG can be output according to the size of the load power.  $D_p$  is the damping coefficient of the active power-frequency loop,  $D_q$  is the droop coefficient of the reactive power-voltage loop,  $k_q$  is the gain of the reactive power-voltage loop,  $u_\alpha$  and  $u_\beta$  are the voltages of the two supply arms respectively, and the voltage phase of the supply arm is obtained through the phase-locked loop (PLL). Thus, the single-phase VSG output voltage phase is controlled to synchronize with the supply arm voltage phase to achieve the purpose of uninterrupted phase-separation passing of the train. The calculated virtual transient electromotive force  $e$  is used as the modulated wave signal to the PWM wave module. Voltage phase control can control the phase of single-phase VSG output voltage.

The model of the MAF is shown in Fig. 5. The MAF is composed of an integral link, delay link, and gain link.

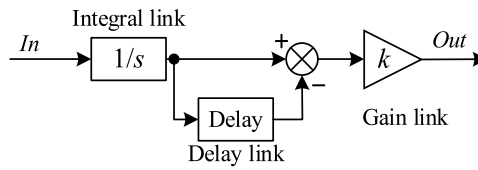


Fig. 5. Schematic diagram of MAF

### 3.3. Energy management strategy

The energy storage system gives priority to whether there is a train passing the electric phase separation. If there is a train passing the electric phase-separation, the energy storage system gives priority to providing power to the over-electric phase-separation train. The energy management strategy of the RPC-SCESSS is shown in Fig. 6.  $I_{limL}$ ,  $I_{limH}$  is the charging and discharging

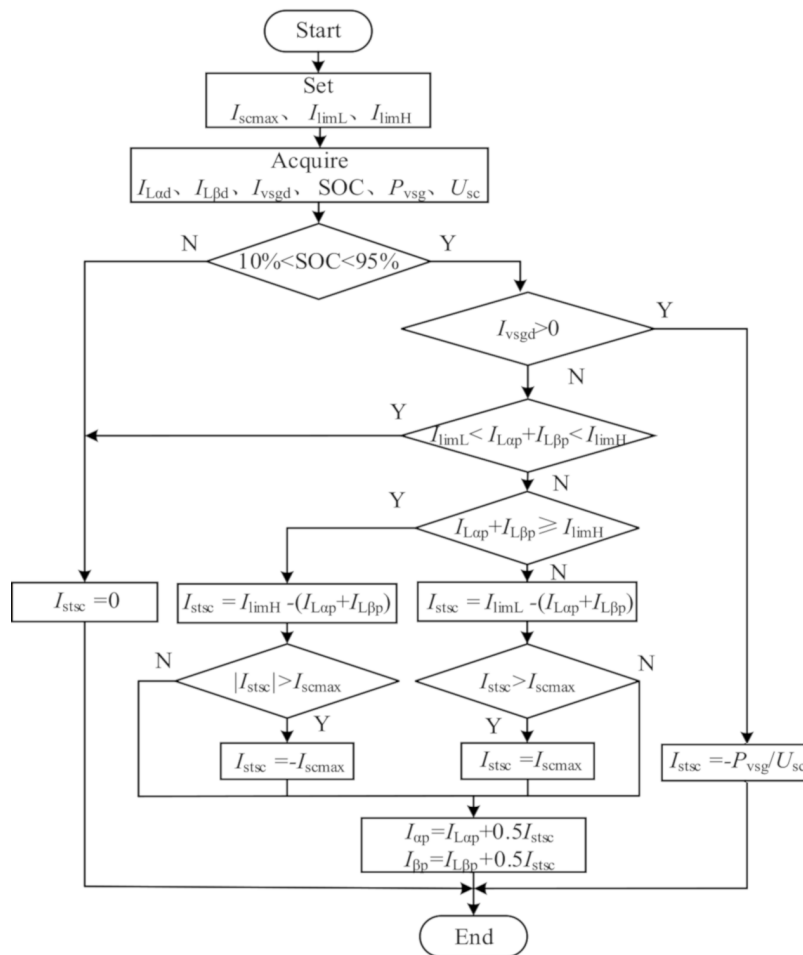


Fig. 6. Flowchart of the RPC-SCESSS energy management policy



threshold of the energy storage system.  $I_{vsgd}$  is a single-phase VSG output active current.  $U_{SC}$  is the voltage at both ends of the supercapacitor.

## 4. Simulation analysis

### 4.1. System parameters

In Matlab/Simulink, the overall model of the UPSP system based on the RPC–SCESS is built and simulated. The system parameters are shown in Table 1.

Table 1. System parameters

System type	Parameters name	Parameters
Traction substation	V/v transformer ratio $k_T$	220/27.5
	Substation capacity/MVA	40
	$T_\alpha, T_\beta$ Step-down transformer ratio $k$	27.5/1.5
Railway power regulator (RPC)	RPC device capacity $S_{C \max}$ /MVA	4
	Filter inductance $L_s$ /H	0.6e-3
	Support capacitance $C_d$ /F	10e-3
	Intermediate DC side voltage $U_{dc}$ /V	3 100
Energy storage system (ESS)	DC/DC device capacity $P_{st \max}$ /MW Energy storage medium	2 supercapacitor
	Energy storage capacity/MWh	0.07
	Capacity of the supercapacitor/F	140
Single-phase VSG system	$T_{vsg}$ Transformer ratio $k_{vsg}$	27.5/1.5
	Filter inductance $L_1$ /mH	0.7
	Filter inductance $L_2$ /mH	0.01
	Filter capacitance $C_f$ /mF	0.01
	Passive damping $R_d$ / $\Omega$	0.3
	Support capacitance $C_1, C_2$ /F	5e-3
	Damping coefficient $D_p$	2 000
	Virtual inertia $J$ /kg·m <sup>2</sup>	0.01
	Sagging coefficient $D_q$	3 750
	Gain $k_q$	$2.7 \times 10^5$
	MAFT <sub>delay</sub> /s	0.02
	MAF gain $k$	50
PWM carrier frequency $f_{sw}$ /kHz	5	
Load power	Active power/ W	1e6
	Reactive power/ Var	1e5

### 4.2. Simulation result

Set the train to pass the electric phase-separation at 0.5 s, transform the neutral line voltage at 1.5 s, and end the electric over phase-separation at 2 s. The voltage and current of the neutral line are shown in Fig. 7.

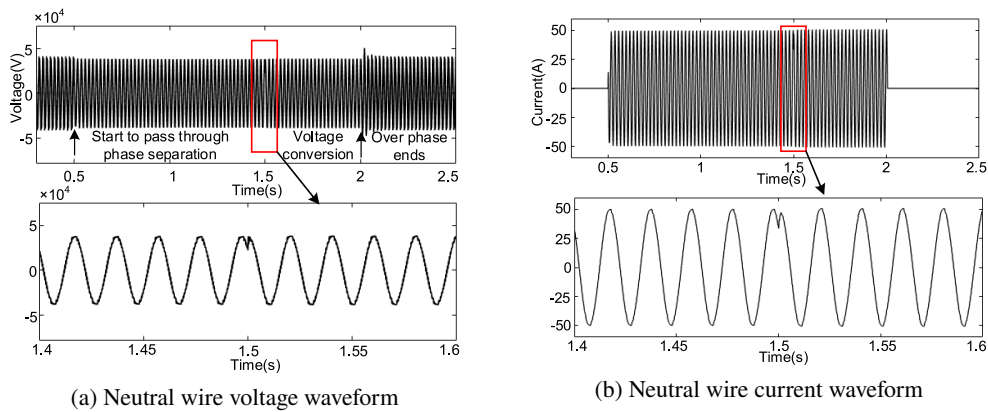


Fig. 7. Neutral line voltage and current waveform

When the voltage switches at 1.5 s, the voltage between the neutral region and the two supply arms is shown in Fig. 8. As can be seen from Fig. 8, before 1.5 s, the phase of the neutral zone voltage is consistent with the phase of the  $\alpha$  supply arm voltage, allowing the train to transition from the  $\alpha$  supply arm to the neutral zone. When the voltage is converted at 1.5 s, the voltage in the neutral region can be transformed in one cycle, keeping the phase consistent with the  $\beta$  power supply arm, to ensure that the train can safely transition from the neutral region to the  $\beta$  power supply arm.

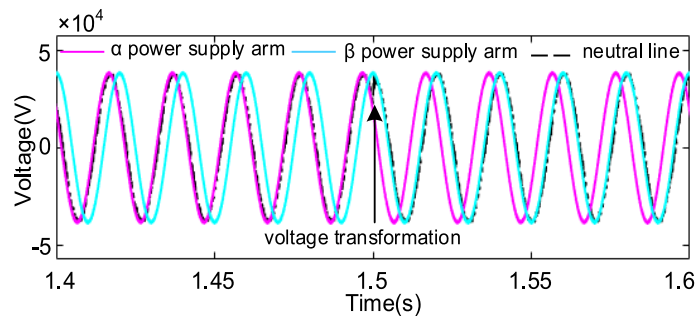


Fig. 8. Two supply arms and neutral wire voltage waveforms

The output power of the single-phase VSG is shown in Fig. 9. It can be seen from Fig. 9 that the single-phase VSG can precisely output according to the active and reactive power required by the load.

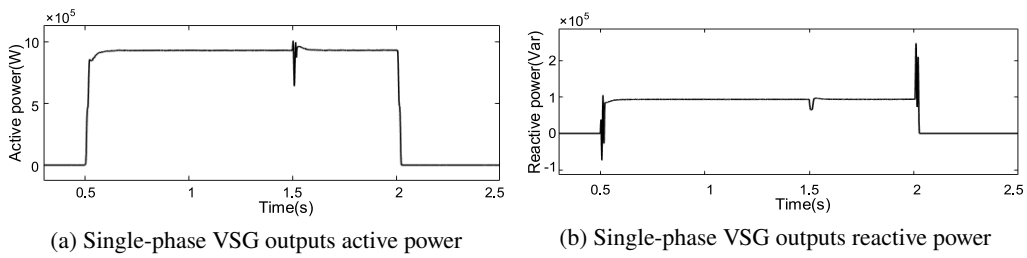


Fig. 9. Single-phase VSG output power

When the energy storage system does not work, the single-phase VSG output power is transmitted by two power supply arms through the RPC, as shown in Fig. 10.

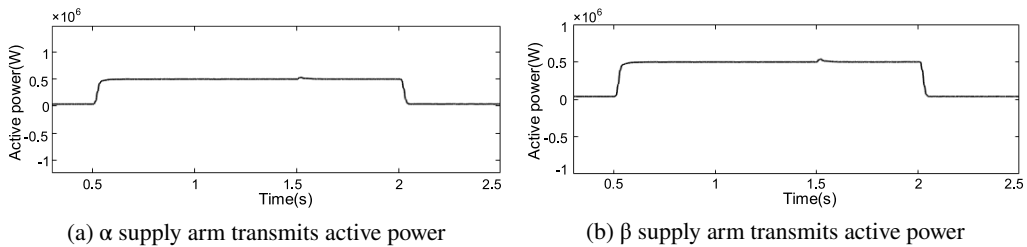


Fig. 10. RPC transfers power when the energy storage system is not operating

When the energy storage system works, the single-phase VSG output power is provided by the supercapacitor energy storage system, and the RPC does not carry out power transmission at this time, as shown in Fig. 11.

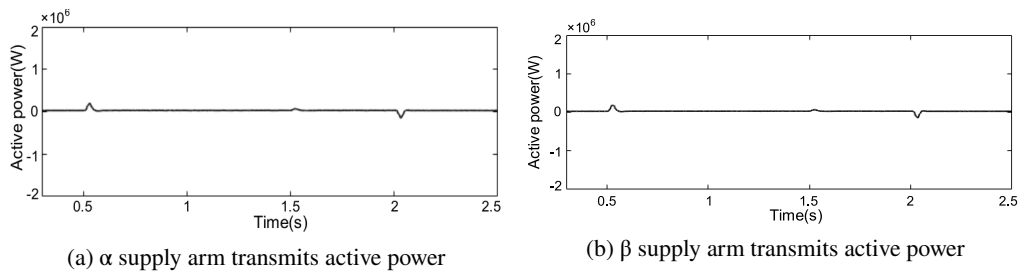


Fig. 11. RPC transfer power during energy storage system operation

The initial state of charge of the supercapacitor is 75%. When the train begins to phase out, the supercapacitor discharges and the state of charge decreases, as shown in Fig. 12. The intermediate DC side voltage of the RPC is shown in Fig. 13.

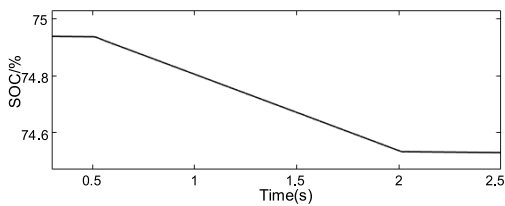


Fig. 12. Supercapacitor charge state

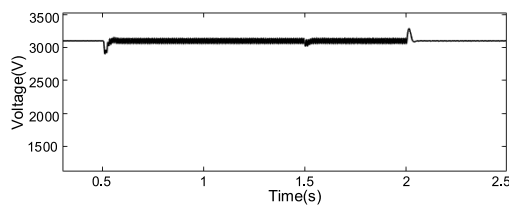


Fig. 13. RPC intermediate DC side voltage

The frequency of the neutral region is supported by the single-phase VSG, and the output frequency of the single-phase VSG is shown in Fig. 14. It can be seen from Fig. 14 that the frequency of the neutral region meets the frequency requirements of the traction network.

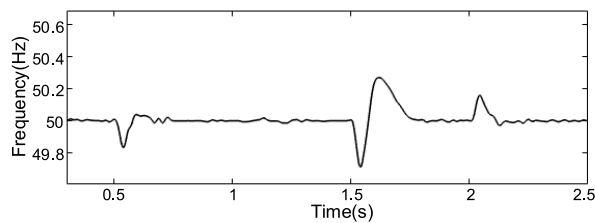


Fig. 14. Single-phase VSG output frequency

## 5. Conclusions

This paper establishes an RPC–SCESS based UPSP system, and the single-phase inverter has the advantages of simple structure and low cost. The single-phase VSG control provides voltage and frequency support for the neutral zone to meet the power demand of the train during pass electric phase-separation. The simulation results show that the proposed scheme can realize constant electric power throughout the whole process of train pass electric phase-separation, so as to effectively avoid the safety pass electric phase-separation problem caused by train deceleration in the long ramp uphill section, and uses the braking energy for the train over the electrical phase-separation process, which improves the utilization rate of regenerative braking energy. The power allocation and capacity optimization between the UPSP system and the RPC–SCESS will be the focus of future research.

### Acknowledgements

This work was supported in part by the National Natural Science Foundation of China (52067013). The Natural Science Key Fund Project of the Gansu Provincial Department of Science and Technology (21JR7RA280, 22JR5RA318, 22JR11RA162). Ministry (KFKT2020-12), the Tianyou Innovation Team Science Foundation of intelligent power supply and state perception for rail.

**References**

- [1] Hu J.X., Zhou F.Y., *Status quo and development of train phasing technology for electrified railway*, Electric Drive for Locomotive, no. 3, pp. 1–5 (2019), DOI: [10.13890/j.issn.1000-128x.2019.03.001](https://doi.org/10.13890/j.issn.1000-128x.2019.03.001).
- [2] Deng Y.C., Lin Z.L., *Challenges and Countermeasures for the Electrification Project of Sichuan-Tibet Railway*, Electrified Railway, vol. 30, no. S1, pp. 5–11+15 (2019), DOI: [10.19587/j.cnki.1007-936x.2019z.002](https://doi.org/10.19587/j.cnki.1007-936x.2019z.002).
- [3] Li Y.J., *Research on uninterrupted phase-separation passing technology of high-speed railway bullet trains*, Western Transportation Science and Technology, vol. 2, no. 4 (2020), DOI: [10.13282/j.cnki.wccst.2020.02.040](https://doi.org/10.13282/j.cnki.wccst.2020.02.040).
- [4] Li Q.Z., *Some key Technical Problems in the development of high-speed Railway traction Power supply*, Journal of the China Railway Society, vol. 32, no. 4, pp. 119–124 (2010), DOI: [10.3969/j.issn.1001-8360.2010.04.022](https://doi.org/10.3969/j.issn.1001-8360.2010.04.022).
- [5] Hu H.T., Meng X., Yang X.W., *Research on hierarchical control strategy of new 24kV flexible DC railway traction power supply system*, Chinese Journal of Electrical Engineering, vol. 41, no. 10, pp. 3373–3382, 3663 (2021), DOI: [10.13334/j.0258-8013.pcsee.200379](https://doi.org/10.13334/j.0258-8013.pcsee.200379).
- [6] Tian X., Jiang Q.R., Wei Y.D., *Study on the Scheme of Electrified Railway Passing Phase Separation without Power Failure*, Power System Protection and Control, vol. 40, no. 21, pp. 14–18 (2012), DOI: [10.3969/j.issn.1674-3415.2012.21.003](https://doi.org/10.3969/j.issn.1674-3415.2012.21.003).
- [7] Tian X., Jiang Q.R., Wei Y.D., *Topological research on continuous current passing through phase separation device of electrified railway based on two-phase modular multilevel converter*, Grid Technology, vol. 39, no. 10, pp. 2901–2906 (2015), DOI: [10.13335/j.1000-3673.pst.2015.10.033](https://doi.org/10.13335/j.1000-3673.pst.2015.10.033).
- [8] Wang W.F., Li Z.X., Zhao C., *Research on the control strategy of a non-full capacity continuous current passing phase separation device*, Chinese Journal of Electrical Engineering, vol. 39, no. 5, pp. 1461–1470 (2019), DOI: [10.13334/j.0258-8013.pcsee.180497](https://doi.org/10.13334/j.0258-8013.pcsee.180497).
- [9] Huang Y., Hu H.T., Wang Y.Y., *Electrified railway train flexible continuous electric passing split phase system and its control strategy*, Journal of Electrical Technology, vol. 36, no. 23, pp. 4959–4969 (2021), DOI: [10.19595/j.cnki.1000-6753.tces.210874](https://doi.org/10.19595/j.cnki.1000-6753.tces.210874).
- [10] Hu H.T., Chen J.Y., Ge Y.B., *Research on regenerative braking energy storage and utilization technology of high-speed railway*, Chinese Journal of Electrical Engineering, vol. 40, no. 1, pp. 246–256+391 (2020), DOI: [10.13334/j.0258-8013.pcsee.190650](https://doi.org/10.13334/j.0258-8013.pcsee.190650).
- [11] Mahdiyeh K., Ahmed A.M., Werner B., *Recuperation of regenerative braking energy in electric rail transit systems*, IEEE Transactions on Intelligent Transportation Systems, vol. 20, no. 8, pp. 2831–2847 (2019), DOI: [10.1109/TITS.2018.2886809](https://doi.org/10.1109/TITS.2018.2886809).
- [12] Wang Y., He Y.Q., Chen X.Q., *A layered compensation optimization strategy of energy storage type railway power conditioner*, Archives of Electrical Engineering, vol. 71, no. 1, pp. 5–20 (2022), DOI: [10.24425/aee.2022.140194](https://doi.org/10.24425/aee.2022.140194).
- [13] Lv Z.P., Sheng W.X., Liu H.T., *Application and challenges of virtual synchronous machine technology in power system*, Chinese Journal of Electrical Engineering, vol. 37, no. 2, pp. 349–360 (2017), DOI: [10.13334/j.0258-8013.pcsee.161604](https://doi.org/10.13334/j.0258-8013.pcsee.161604).
- [14] Zhang X., Hu Y.H., Mao W., *A grid-supporting strategy for cascaded H-bridge PV converter using VSG algorithm with modular active power reserve*, Industrial Electronics, IEEE Transactions on Industrial Electronics, vol. 68, no. 11, pp. 186–197 (2021), DOI: [10.1109/TIE.2019.2962492](https://doi.org/10.1109/TIE.2019.2962492).
- [15] Chen X.D., Ge X., Diao F., *Control strategy of traction rectifier based on virtual synchronous machine*, Electronics Letters, vol. 54, no. 7, pp. 433–435 (2018), DOI: [10.1049/el.2017.2922](https://doi.org/10.1049/el.2017.2922).

- [16] Chen J.X., Wang Y., Chen X.Q., *A vehicle-mounted energy storage solution considering voltage fluctuation and harmonic control of traction network in mountainous areas*, Journal of Railway Science and Engineering, vol. 18, no. 6, pp. 1582–1594 (2021), DOI: [10.19713/j.cnki.43-1423/u.T20200793](https://doi.org/10.19713/j.cnki.43-1423/u.T20200793).
- [17] Zhang M.S., Chi B.X., Li J.W., *Research on current coordinated control strategy of active power filter based on quasi-proportional resonance*, Grid Technology, vol. 43, no. 5, pp. 1614–1623 (2019), DOI: [10.13335/j.1000-3673.pst.2018.0762](https://doi.org/10.13335/j.1000-3673.pst.2018.0762).
- [18] Gao B.T., Xia C.P., Zhang L., *VSC-HVDC rectifier side modeling and parameter design based on virtual synchronous motor technology*, Chinese Journal of Electrical Engineering, vol. 37, no. 2, pp. 534–54 (2017), DOI: [10.13335/j.1000-3673.pst.2018.0762](https://doi.org/10.13335/j.1000-3673.pst.2018.0762).
- [19] Li H., Zhang X.C., Shao T.C., *Flexible inertia optimization for single-phase voltage source inverter based on hold filter*, IEEE Journal of Emerging and Selected Topics in Power Electronics, vol. 7, no. 2, pp. 1300–1310 (2019), DOI: [10.1109/JESTPE.2018.2865214](https://doi.org/10.1109/JESTPE.2018.2865214).
- [20] Yu J.R., Sun W., Yu J.Q., *Virtual synchronous generator control of grid-connected inverter based on inertia adaptive*, Power System Protection and Control, vol. 50, no. 4, pp. 137–144 (2022), DOI: [10.19783/j.cnki.pspc.210775](https://doi.org/10.19783/j.cnki.pspc.210775).
- [21] Cui J.T., Li Z., He P., *Electromechanical transient modeling of energy storage based on virtual synchronous machine technology*, Archives of Electrical Engineering, vol. 71, no. 3, pp. 581–599 (2022), DOI: [10.24425/aee.2022.141672](https://doi.org/10.24425/aee.2022.141672).
- [22] Ren T.R., Yu X.N., Tong S.F., *Design and evaluation of high sensitivity underwater optical communication transceiver based on digital signal processing*, China Laser, vol. 49, no. 4, pp. 107–116 (2022), DOI: [10.3788/CJL202249.0406005](https://doi.org/10.3788/CJL202249.0406005).